Journal of Inorganic Biochemistry 106 (2012) 156–163

Contents lists available at SciVerse ScienceDirect

Journal of Inorganic Biochemistry

journal homepage: www.elsevier.com/locate/jinorgbio

Synthesis, characterization, crystal structures and *in vitro* antistaphylococcal activity of organotin(IV) derivatives with 5,7-disubstituted-1,2,4-triazolo[1,5-a]pyrimidine

Maria Assunta Girasolo [a,*], Loredana Canfora [a], Piera Sabatino [b], Domenico Schillaci [c], Elisabetta Foresti [b], Simona Rubino [a], Giuseppe Ruisi [a], Giancarlo Stocco [a]

[a] Dipartimento di Chimica "Stanislao Cannizzaro", Università di Palermo, Viale delle Scienze, I-90128 Palermo, Italy
[b] Dipartimento di Chimica G. Ciamician,Università di Bologna,via F. Selmi 2, 40126 Bologna, Italy
[c] Dipartimento di Scienze e Tecnologie Molecolari e Biomolecolari, Università di Palermo, via Archirafi 32, I-90123 Palermo, Italy

ARTICLE INFO

Article history:
Received 7 June 2011
Received in revised form 6 September 2011
Accepted 6 September 2011
Available online 14 September 2011

Keywords:
Triazolopyrimidine
Organotin(IV)
X-ray-structure
^{119}Sn Mössbauer
Antimicrobial activity

ABSTRACT

New organotin(IV) complexes of 5,7-ditertbutyl-1,2,4-triazolo[1,5-a]pyrimidine (**dbtp**) and 5,7-diphenyl-1,2,4-triazolo[1,5-a]pyrimidine (**dptp**) with 1:1 and/or 1:2 stoichiometry were synthesized and investigated by X-ray diffraction, FT-IR and ^{119}Sn Mössbauer in the solid state and by ^{1}H and ^{13}C NMR spectroscopy, in solution. Moreover, the crystal and molecular structures of $Et_2SnCl_2(dbtp)_2$ and $Ph_2SnCl_2(EtOH)_2(dptp)_2$ are reported. The complexes contain hexacoordinated tin atoms: in $Et_2SnCl_2(dbtp)_2$ two 5,7-ditertbutyl-1,2,4-triazolo[1,5-a]pyrimidine molecules coordinate classically the tin atom through N(3) atom and the coordination around the tin atom shows a skew trapezoidal structure with axial ethyl groups. In $Ph_2SnCl_2(EtOH)_2(dptp)_2$ two ethanol molecules coordinate tin through the oxygen atom and the 5,7-diphenyl-1,2,4-triazolo[1,5-a]pyrimidine molecules are not directly bound to the metal center but strictly H-bonded, through N(3), to the –OH group of the ethanol moieties; $Ph_2SnCl_2(EtOH)_2(dptp)_2$ has an all-trans structure and the C–Sn–C fragment is linear. On the basis of Mössbauer data, the 1:2 diorganotin(IV) complexes are advanced to have the same structure of $Et_2SnCl_2(dbtp)_2$, while $Me_2SnCl_2(dptp)_2$ to have a regular all-trans octahedral structure. A distorted *cis*-R_2 trigonal bipyramidal structure is assigned to 1:1 diorganotin(IV) complexes. The *in vitro* antibacterial activities of the synthesized complexes have been tested against a group of reference pathogen micro-organisms and some of them resulted active with MIC values of 5 μg/mL, most of all against staphylococcal strains, which shows their inhibitory effect.

© 2011 Elsevier Inc. All rights reserved.

1. Introduction

Triazolopyrimidine derivatives are well known N-donor heterocyclic ligands [1,2]; the steric effects of substituents in these ligands are interesting and have not been explored in great details for organotins, especially for those ligands bearing substituents at positions 5 and 7, while triazolopyrimidine and its derivatives have gained great attention as ligands to transition metals [3–6]. Our interest was recently devoted to organotin(IV) complexes of [1,2,4] triazolo-[1,5-a]pyrimidine (tp), its 5,7-dimethyl derivative (dmtp) and a number of oxo-substituted triazolopyrimidines whose antimicrobial activity was excellent [7–9]. This promising finding was suggesting a possible use of triazolopyrimidines derivatives as leads for a potential field of novel therapeutic options able to overcome the antibiotic resistant strains which prompted us to undertake the present study by evaluating the change of activity associated with the introduction on the basic heterocycle of different radical groups giving non classical isosteric ligands, expected to be endowed with better hydrophobicity. Besides, organotins are known to possess, *per se*, antitumour [10,11], antimicrobial [12] and anti-inflammatory [13] activities; triazolopyrimidines complexes with several divalent metal ions have been tested as inhibitors of the growth of different Gram(+) and Gram(−) bacteria [12]. In particular, recent findings on compounds of metal ions (Co(II), Cu(II), Ni(II)) with closely related ligands, have proven to be effective antiparasital agents against *Trypanosoma cruzi* [14] and to be endowed with antiproliferative *in vitro* activity against *Leishmania* spp. [15]; the biological activity on these specimen is still in progress [16]. Staphylococci can induce a wide spectrum of infectious diseases associated with remarkable morbidity and mortality [17]. Pathogenic staphylococci have also an amazing ability to acquire resistance traits to antibiotics, the rise of community and hospital-acquired methicillin resistant *Staphylococcus aureus* (MRSA) being a major health problem that has created a pressing need for novel therapeutic options [18]. The threat of pathogenic bacteria resistant to most or all conventional antibiotics could be faced by developing new antibacterial agents with a different mode of action than those of traditional antibiotics. In this paper we report the synthesis and characterization of organotin (IV) adducts (R_2SnCl_2, R = Me, Et, *n*-Bu and Ph and $RSnCl_3$, R = *n*-Bu) with 5,7-ditertbutyl-1,2,4-triazolo[1,5-a]pyrimidine (**dbtp**) and 5,7-

* Corresponding author. Tel.: +39 091 6575524; fax: +39 091 427584.
E-mail address: assunta.girasolo@unipa.it (M.A. Girasolo).

0162-0134/$ – see front matter © 2011 Elsevier Inc. All rights reserved.
doi:10.1016/j.jinorgbio.2011.09.010

diphenyl-1,2,4-triazolo[1,5-a]pyrimidine (**dptp**) (Fig. 1) in a 1:1 and 1:2 molar ratio. The crystal and molecular structures of $Et_2SnCl_2(dbtp)_2$ and $Ph_2SnCl_2(EtOH)_2(dptp)_2$ are also reported and their metal-to-triazolo pyrimidine ligand interaction is discussed, together with their overall supramolecular organization. We tested the biological activity of all the specimen against a group of staphylococcal reference strains (*S. aureus* ATCC 25923, *S. aureus* ATCC 29213, methicillin resistant *S. aureus* 43866 and *S. epidermidis* RP62A) along with Gram-negative pathogens (*P. aeruginosa* ATCC9027 and *E. coli* ATCC25922).

2. Experimental

2.1. Materials and methods

The chemicals used throughout in the present study were purchased from C. Erba (Milan, Italy), Sigma-Aldrich (Milan, Italy), and Merck KGaA (Germany), and used without further purification. Anhydrous methanol was obtained by standard procedure. Elemental microanalyses for C, H and N were carried out by the Laboratorio di Microanalisi, University of Padova, Italy. Chlorine was determined by potentiometric titration with standard silver nitrate after combustion in pure oxygen according to Schöniger [19]. Tin was gravimetrically determined as SnO_2. Infrared spectra (nujol mulls, CsI windows) were recorded with an FT-IR spectrometer Perkin-Elmer Spectrum One. The Mössbauer (nuclear γ resonance) spectrometers, the related instrumentation and data reduction procedures were as previously described [20]. A 10 mCi $Ca^{119}SnO_3$ source (RITVERC GmbH, St. Petersburg, Russia) was employed. The isomer shifts (δ) are relative to room temperature $Ca^{119}SnO_3$. The ^1H and ^{13}C NMR spectra were acquired in $CDCl_3$ solutions at 298 K on a Bruker 300 Avance spectrometer at 300.13 and 75.47 MHz, respectively.

2.2. X-ray crystal determination

Suitable crystals of $Ph_2SnCl_2(EtOH)_2(dptp)_2$ for the X-ray diffraction studies were grown from ethanol, data collection was made on a BRUKER AXS SMART 2000 CCD diffractometer using graphite-monochromated MoKα radiation (λ = 0.71073 Å). Data were collected using 0.3° wide ω scans and a crystal-to-detector distance of 5.0 cm and corrected for absorption empirically using the SADABS routine [21]. Data collection nominally covered a full sphere of reciprocal space with 30 s exposure time per frame. The SAINT [22] program was used for analysis of the data reduction and revealed a monoclinic P21/c space group. The structure was solved by direct Methods using the SHELXS-97 [23] program and refined on F^2 by full matrix least-squares calculations using the SHELXTL package. The anisotropy parameters of non-H atoms were refined with the SHELXL-97 [24] program. All H atoms of ligands were geometrically included in the refinement, and refined "riding" on their corresponding carbon or oxygen atom, except for the H atom connected to the O (1) atom, which was found experimentally in a difference Fourier map after all the "heavy" atoms were located [C–H 0.93 Å and 0.97 Å for aromatic and aliphatic distances; OH 0.82 Å]. Thermal vibrations were treated anisotropically. In addition, the refinement used theta range for data collection between 2.9 and 30.00° and show final R indices $R_1 = 0.0375$ for 4307 reflections with Fo>4sig (Fo) and 0.0540 for all 5469 data, $wR_2 = 0.1234$, GooF = S = 0.758, restrained GooF = 0.758 for all data.

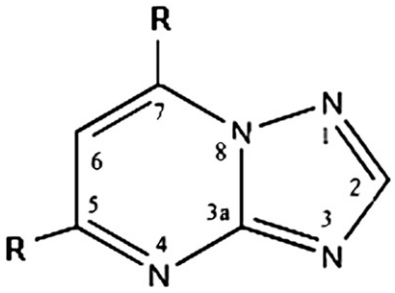

Fig. 1. The ligand molecules with the atom numbering scheme: R = $C(CH_3)_3$ (**dbtp**) and R = C_6H_5 (**dptp**).

For $Et_2SnCl_2(dbtp)_2$, suitable crystals were grown from diethyl ether; the X-ray diffraction data were collected at 295 K using an Oxford Xcalibur S with Mo–Kα radiation, λ = 0.71073 Å, monochromator graphite for $Et_2SnCl_2(dbtp)_2$. The cell parameters for the molecule were obtained and refined, respectively, catching reflections with random orientation in hkl planes. Intensities were corrected by Lorentz polarization and absorption with the SADABS [21] program. The SAINT [22] program was used for analysis of the data reduction and revealed a monoclinic $P2_1/c$ space group. The structure was solved by direct methods using the SHELXS-97 [23] program. The anisotropy parameters of non-H atoms were refined with the SHELXL-97 [24] program. All H atoms of ligands were geometrically included in the refinement. Aromatic carbons were refined with Uiso(H) = 1.2 Ueq Csp2 and methyl carbons with Uiso(H) = 1.5 Ueq Csp3. In addition, the final refinement used the complete theta range for data collection between 2.9 and 30.00° and shows final R indices $R_1 = 0.0376$ for 2604 reflections with Fo>4sig(Fo) and 0.0900 for all 4317 data, $wR_2 = 0.0800$, GooF = S = 0.804, restrained GooF = 0.804 for all data. X-ray data are listed in Table 1. ORTEP-3 [25] for Windows was used to draw the figures while Mercury was used for the graphical representation of the crystal packings [26]. Analysis of crystal data was performed through PARST [27].

2.3. Antimicrobial activity

2.3.1. Bacterial strains

A group of staphylococcal reference strains, *viz. S. aureus* ATCC 25923, *S. aureus* ATCC 29213 and methicillin resistant *S. aureus*

Table 1
Crystal data and details of refinement for $Et_2SnCl_2(dbtp)_2$ (***4***) and $Ph_2SnCl_2(EtOH)_2(dptp)_2$(***11***).

Compound	4	11
Empirical formula	$C_{30}H_{50}Cl_2N_8Sn$	$C_{50}H_{46}C_{l2}N_8O_2Sn$
Formula weight	712.37	980.54
Temperature (K)	293 K	293 K
Wavelength (Å)	0.71073	0.71073
Crystal system	Monoclinic	Monoclinic
Space group	$P2_1/c$	I2/a
a (Å)	17.8248(5)	13.4604(6)
b (Å)	11.1062(2)	7.7689(4)
c (Å)	18.4027(5)	22.3827(10)
β (°)	101.818(3)	106.4490(10)
Volume (Å^3)	3565.88(15)	2244.82(18)
Z	4	2
Density (Mg m^{-3})	1.327	1.451
F(000)	1480	1004
Crystal size (mm)	0.15×0.30×0.22	0.35×0.20×0.30
θ Range for data collection (°)	2.90–29.50	1.90–28.73
Index range	$-24 \le h \le 24$ $-14 \le k \le 14$, $-24 \le l \le 25$	$-17 \le h \le 17$ $-10 \le k \le 10$, $-30 \le l \le 29$
Reflections collected	19553	25299
Data/restraints/parameters	4317/0/178	5469/0/256
Goodness-of-fit on F^2	0.804	0.757
Final *R* indices [$I>2\sigma(I)$]	$R_1 = 0.0376$, $wR_2 = 0.0676$	$R_1 = 0.0375$, $wR_2 = 0.1075$
Largest diff. peak and hole (e Å^{-3})	0.28–0.36	0.51–0.49

43866 and *S. epidermidis* RP62A was used. Two important Gram-negative reference strains were also used: *Pseudomonas aeruginosa* ATCC 9027 and *Escherichia coli* ATCC 25922.

2.3.2. Determination of MICs

Minimum inhibitory concentrations (MICs) against tested strains were determined as previously described by a broth dilution micromethod [28]. A series of solutions with a range of concentrations from 40 to 0.1 μg/mL (obtained by twofold serial dilution) was made in Mueller-Hinton broth (Merck) in a 96-well plate. To each well 10 μL of a bacterial suspension, obtained from a 24 h culture, containing ~10^6 colony forming units (CFU)/mL were added. The plate was incubated at 37 °C for 24 h. After this time the MIC values were determined by a microplate reader (ELX 800, Bio-Tek Instruments) as the lowest concentration of compound whose optical density (OD) at 570 nm, was comparable to the negative control wells (broth only). Amikacin was used for comparative and quality control purposes.

2.4. Synthesis of ligands

The ligands **dbtp** and **dptp** were synthesized following the Grodzicki [29] procedure with some modifications: in both cases 10 mmol of the chemicals (3-amino-1,2,4-triazole and 2,2,6,6-tetramethylheptane-3,5-dione or 1,3-diphenylpropane-1,3-dione respectively) and 5 mL of 85% H_3PO_4 in H_2O were refluxed for 24 h, then the reaction mixture was cooled at room temperature and treated as reported by Grodzicki.

2.5. Synthesis of dbtp adducts

Diorganotin(IV)dichloride-dbtp adducts were prepared reacting the organometallic compound (1 mmol) with **dbtp** (1 or 2 mmol) in diethyl ether (20 mL). After reducing the volume of the clear reaction mixture in air, 1:1 or 1:2 solid adducts were obtained depending on the reaction ratio. *n*-$BuSnCl_3$ gave the 1:2 adduct independently of the reaction ratio: a bulky precipitate is formed immediately after mixing the reagents. The complexes were recrystallized from diethyl ether. Single crystals of $Et_2SnCl_2(dbtp)_2$ suitable for X-ray diffraction studies were obtained by slow evaporation of diethyl ether solution at room temperature.

2.5.1. $Me_2SnCl_2(dbtp)$ (**1**) and $Me_2SnCl_2(dbtp)_2$ (**2**)

$C_{15}H_{26}Cl_2N_4Sn$ (452.02) (***1***), m.p.152–154 °C; Anal. Calc.: C, 39.86; H, 5.80; N, 12.39; Cl, 15.69; Sn, 26.26. Found: C, 39.81; H, 6.02; N, 12.31; Cl, 15.06; Sn, 25.52%. Selected IR data (CsI, cm^{-1}):1615 s (strong) (ν_{tp}), 1532 s (ν_{py}), 576 m (medium) ν_{as}(Sn–C); 520w (weak) ν_s(Sn–C); 322 s ν_{as}(Sn–Cl); 273 s ν_s(Sn–Cl). ^{1}H NMR ($CDCl_3$): δ (ppm) = 8.58 (s (singlet), 1H, H-2), 7.11 (s, 1H, H-6), 1.64 (s, 9H, H-5), 1.45 (s, 9H, H-7), 1.30 (s, 6H, Sn–CH_3), $|^2J(^{119}Sn,H)| = 78.8$ Hz ∠C–Sn–C = 127.7°, $|^2J(^{117}Sn,H)| = 75.6$ Hz ∠C–Sn–C = 125.6°. ^{13}C NMR ($CDCl_3$): δ (ppm) = 152.9 (C-2), 154.3 (C-3a), 177.4 (C-5), 104.6 (C-6), 158.6 (C-7), 36.7, 39.2, 27.2, 29.8 (C(CH_3)$_3$); 10.8 (Sn–CH_3). ^{119}Sn Mössbauer data: δ = 1.37, ΔE = 3.46, Γ± = 0.83 mm s^{-1}, ∠C–Sn–C = 132°. $C_{28}H_{46}Cl_2N_8Sn$ (684.35) (***2***); m.p. 142–144 °C. Anal. Calc.: C, 49.14; H, 6.78; N, 16.37; Cl, 10.36; Sn, 17.35. Found: C, 49.28; H, 6.75; N, 16.85; Cl, 10.73; Sn, 17.33%. Selected IR data (CsI, cm^{-1}):1615 s (ν_{tp}), 1535 s (ν_{py}), 579 m ν_{as}(Sn–C); 261 s ν_{as}(Sn–Cl). ^{1}H NMR ($CDCl_3$): δ (ppm) = 8.52 (s, 1H, H-2), 7.07 (s, 1H, H-6), 1.63 (s, 9H, C(CH_3)$_3$), 1.45 (s, 9H, C(CH_3)$_3$), 1.31 (s, 6H, Sn–CH_3), $|^2J(^{119}Sn,H)| = 80.4$ Hz ∠C–Sn–C = 131.4°, $|^2J(^{117}Sn,H)| = 76.96$ Hz ∠C–Sn–C = 127.2°. ^{13}C NMR ($CDCl_3$): δ (ppm) = 153.4 (C-2), 155.7 (C-3a), 176.8 (C-5), 104.2 (C-6), 158.3 (C-7); 36.6, 39.1, 27.2, 29.8 (C(CH_3)$_3$); 12.5 (Sn–CH_3). ^{119}Sn Mössbauer data: δ = 1.37, ΔE = 3.90, Γ± = 0.79 mm s^{-1}, ∠C–Sn–C = 158°.

2.5.2. $Et_2SnCl_2(dbtp)$ (**3**) and $Et_2SnCl_2(dbtp)_2$ (**4**)

$C_{17}H_{30}Cl_2N_4Sn$ (480.07) (***3***); m.p. 83–85 °C. Anal. Calc.: C, 42.53; H, 6.30; N, 11.67; Cl, 14.77; Sn, 24.73. Found: C, 42.94; H, 6.36; N, 12.01; Cl, 15.08; Sn, 25.15%. Selected IR data (CsI, cm^{-1}):1615 s (ν_{tp}), 1531 s (ν_{py});540 m ν_{as}(Sn–C); 499 m ν_s(Sn–C); 314 s ν_{as}(Sn–Cl); 269 s ν_s(Sn–Cl). ^{1}H NMR ($CDCl_3$): δ (ppm) = 8.56 (s, 1H, H-2), 7.09 (s, 1H, H-6), 1.63 (s, 9H, C(CH_3)$_3$), 1.45 (s, 9H, C(CH_3)$_3$), 1.84 (q (quartet), 4H, Sn–C_2H_5), $|^2J(^{119}Sn,H)| = 57.8$ Hz ∠C–Sn–C = 110.9°, $|^2J(^{117}Sn,H)| = 55.4$ Hz ∠C–Sn–C = 109.7°, 1.41(t (triplet), 6H, Sn–C_2H_5), $|^3J(^{119}Sn,H)| = 144.1$ Hz, $|^3J(^{117}Sn,H)| = 137.6$ Hz. ^{13}C NMR ($CDCl_3$): δ (ppm) = 153.6 (C-2), 154.7 (C-3a), 177.0 (C-5), 104.4 (C-6), 158.4 (C-7); 36.6, 42.8, 27.2, 29.8 (C(CH_3)$_3$); 21.8 (Sn–C_2H_5), 9.8 (Sn–C_2H_5, $|^2J(^{119}Sn,C)| = 44.2$ Hz).^{119}Sn Mössbauer data: δ = 1.49, ΔE = 3.37, Γ± = 0.78 mm s^{-1}, ∠C–Sn–C = 130°. $C_{30}H_{50}Cl_2N_8Sn$ (712.37) (***4***); m.p. 91–93 °C. Anal. Calc.: C, 50.58; H, 7.07; N, 15.73; Cl, 9.95; Sn, 16.66. Found: C, 50.61; H, 7.03; N, 15.57; Cl, 10.17; Sn 16.84%. Selected IR data (CsI, cm^{-1}):1613 s (ν_{tp}), 1530 s (ν_{py}); 536 m ν_{as}(Sn–C); 495 ν_s(Sn–C); 260 s,br (broad) ν_{as}(Sn–Cl). ^{1}H NMR ($CDCl_3$): δ (ppm) = 8.49 (s, 1H, H-2), 7.04 (s, 1H, H-6), 1.63 (s, 9H, C(CH_3)$_3$), 1.45 (s, 9H, C(CH_3)$_3$), 1.83 (q, 4H, Sn–C_2H_5), $|^2J(^{119}Sn,H)| = 58.6$ Hz ∠C–Sn–C = 111.3°, $|^2J(^{117}Sn,H)| = 56.2$ Hz ∠C–Sn–C = 110.1°, 1.42(t, 6H, Sn–C_2H_5), $|^3J(^{119}Sn,H)| = 144.6$ Hz, $|^3J(^{117}Sn,H)| = 138.4$ Hz. ^{13}C NMR ($CDCl_3$): δ (ppm) = 153.6 (C-2), 154.9 (C-3a), 176.7 (C-5), 104.2 (C-6), 158.2 (C-7); 36.5, 39.0, 27.1, 29.7 (C(CH_3)$_3$); 23.9 (Sn–C_2H_5), 9.9 (Sn–C_2H_5, $|^2J(^{119}Sn,C)| = 48.2$ Hz).^{119}Sn Mössbauer data: δ = 1.57, ΔE = 3.87, Γ± = 0.76 mm s^{-1}, ∠C–Sn–C = 157°.

2.5.3. $Bu_2SnCl_2(dbtp)_2$ (**5**)

$C_{34}H_{58}Cl_2N_8Sn$ (768.51) (***5***); m.p. 61–63 °C. Anal. Calc.: C, 53.14; H, 7.61; N, 14.58; Cl, 9.23; Sn, 15.45. Found: C, 53.51; H, 7.06; N, 14.94; Cl, 9.24; Sn 15.42%. Selected IR data (CsI, cm^{-1}):1615 s (ν_{tp}), 1535 s (ν_{py}); 592 m ν_{as}(Sn–C); 517w ν_{as}(Sn–Cl); 268 m,br ν_s(Sn–Cl). ^{1}H NMR ($CDCl_3$): δ (ppm) = 8.50 (s, 1H, H-2), 7.05 (s, 1H, H-6), 1.62 (s, 9H, C(CH_3)$_3$), 1.44 (s, 9H, C(CH_3)$_3$), 1.86–1.78 m (multiplet), 1.37 m, 0.87 t (18H, Sn-*n*C_4H_9). ^{13}C NMR ($CDCl_3$): δ (ppm) = 153.9 (C-2), 155.3 (C-3a), 176.5 (C-5), 104.0 (C-6), 158.1 (C-7); 36.5, 39.1, 27.2, 29.8 (C(CH_3)$_3$); 26.4, 30.3, 27.4, 13.7 (Sn–*n*C_4H_9). ^{119}Sn Mössbauer data: δ = 1.55, ΔE = 3.89, Γ± = 0.75 mm s^{-1}, ∠C–Sn–C = 158°.

2.5.4. $Ph_2SnCl_2(dbtp)$ (**6**)

$C_{25}H_{30}Cl_2N_4Sn$ (576.16) (***6***); m.p. 107–109 °C. Anal. Calc.: C, 52.12; H, 5.25; N, 9.72; Cl, 12.31; Sn, 20.60. Found: C, 52.02; H, 5.22; N, 9.79; Cl, 12.32; Sn, 20.51%. Selected IR data (CsI, cm^{-1}):1614 s (ν_{tp}), 1532 s (ν_{py}); 282 m ν_{as}(Sn–C); 223 m ν_{as}(Sn–Cl). ^{1}H NMR ($CDCl_3$): δ (ppm) = 8.53 (s, 1H, H-2), 7.01 (s, 1H, H-6), 1.61 (s, 9H, C(CH_3)$_3$), 1.35 (s, 9H, C(CH_3)$_3$), 7.76–7.73 (m, 4H, Sn–C_6H_5 *ortho*, $|^3J(^{119}Sn,C)| = 91.7$ Hz), 7.48 (m, 6H, Sn–C_6H_5 *meta* + *para*). ^{13}C NMR ($CDCl_3$): δ (ppm) = 153.8 (C-2), 155.1 (C-3a), 176.5 (C-5), 104.0 (C-6), 157.9 (C-7); 36.5, 39.0, 27.2, 29.7 (C(CH_3)$_3$); 139.5 (Sn–C_6H_5 *ipso*), 135.2 (Sn–C_6H_5 *ortho*, $|^2J(^{119}Sn,C)| = 64.2$ Hz, $^2J(^{117}Sn,C) = 62.1$ Hz, 129.6 (Sn–C_6H_5 *meta*, $|^3J(^{119}Sn,C)| = 90.2$ Hz, $|^3J(^{117}Sn,C)| = 86.3$ Hz), 131.4 (Sn–C_6H_5 *para*, $|^4J(^{119}Sn,C)| = 19.8$ Hz, $|^4J(^{117}Sn,C)| = 17.8$ Hz). ^{119}Sn Mössbauer data: δ = 1.23 ΔE = 2.77, Γ± = 0.85 mm s^{-1}, ∠C–Sn–C = 125°.

2.5.5. $BuSnCl_3(dbtp)_2$ (**7**)

$C_{30}H_{49}Cl_3N_8Sn$ (746.85) (***7***); m.p. 152–154 °C. Anal. Calc.: C, 48.25; H, 6.61; N, 15.00; Cl, 14.24; Sn, 15.90. Found: C, 48.32; H, 6.89; N, 14.93; Cl, 14.25; Sn, 16.37%. Selected IR data (CsI, cm^{-1}):1615 s (ν_{tp}), 1535 s (ν_{py}); 602w ν_{as}(Sn–C); 311 m, 292 m, 255w ν(Sn–Cl). ^{1}H NMR ($CDCl_3$): δ (ppm) = 8.72 (s, 1H, H-2), 7.1 (s, 1H, H-6), 1.63 (s, 9H, C(CH_3)$_3$), 1.43 (s, 9H, C(CH_3)$_3$), 2.56–1.90 (m, 4H, Sn–*n*C_4H_9), 1.48 (m, 8H, Sn–*n*C_4H_9), 0.90 (t, 6H, Sn–*n*C_4H_9). ^{13}C NMR ($CDCl_3$): δ (ppm) = 152.9 (C-2), 154.0 (C-3a), 177.6 (C-5), 104.8 (C-6), 158.6 (C-7); 36.7, 39.3, 27.4, 29.8 (C(CH_3)$_3$); 25.8, 29.9, 27.6, 13.8 (Sn–*n*C_4H_9). ^{119}Sn Mössbauer data: δ = 1.00, ΔE = 2.06, Γ± = 0.79 mm s^{-1}.

2.6. Synthesis of dptp adducts

$Me_2SnCl_2(dptp)_2$ (***8***) and *n*-$BuSnCl_3(dptp)_2$ (***12***) were obtained by reaction of the organotin(IV) chloride and **dptp** in ethanol: the mixture was refluxed for 2 h giving a clear solution; on cooling to room temperature crystalline products were obtained. Under the same conditions Ph_2SnCl_2 gave the adduct $Ph_2SnCl_2(EtOH)_2(dptp)_2$ (***11***). The compounds (***8***), (***11***) and (***12***) were recrystallized from ethanol. A further treatment of the compounds with diethyl ether at room temperature didn't give any modification in their spectroscopic properties. By a similar procedure, compounds $Et_2SnCl_2(dptp)$ (***9***) and $Bu_2SnCl_2(dptp)$ (***10***) were obtained from diethyl ether solutions.

2.6.1. $Me_2SnCl_2(dptp)_2$ (**8**)

$C_{36}H_{30}Cl_2N_8Sn$ (764.31) (***8***); m.p. 179–181 °C.Anal. Calc.: C, 56.57; H, 3.96; N, 14.66; Cl, 9.28; Sn, 15.53. Found: C, 56.86; H, 4.01; N, 14.66; Cl, 9.08; Sn, 15.50%. Selected IR data (CsI, cm^{-1}):1612 s (ν_{tp}), 1546 s (ν_{py}); 580 m ν_{as}(Sn–C); 248w ν_{as}(Sn–Cl). ^1H NMR ($CDCl_3$): δ (ppm) = 8.60 (s, 1H, H-2), 7.72 (s, 1H, H-6), 7.66–7.57 (m, 5H, C_6H_5), 8.27–8.12 (m, 5H, C_6H_5), 1.34 (s, 6H, Sn–CH_3), $^2J(^{119}Sn,H)$: 77.4 Hz ∠C–Sn–C = 127.7°, $^2J(^{117}Sn,H)$: 74.0 Hz ∠C–Sn–C = 122.9°. ^{13}C NMR ($CDCl_3$): δ (ppm) = 156.4 (C-2), 155.8 (C-3a), 162.4 (C-5), 107.1 (C-6), 148.6 (C-7), 128.0,129.6 (C_{ortho}), 129.4, 129.3 (C_{meta}), 131.9, 132.3 (C_{para}), 130.0, 136.3 (C_{ipso}), 10.4 (Sn–CH_3). ^{119}Sn Mössbauer data: δ = 1.40, ΔE = 4.17, $\Gamma\pm$ = 0.75 mm s^{-1}, ∠C–Sn–C = 180°.

2.6.2. $Et_2SnCl_2(dptp)$ (**9**)

$C_{21}H_{22}Cl_2N_4Sn$ (520.0) (***9***); m.p. 153–155 °C. Anal. Calc.: C, 48.50; H, 4.26; N, 10.77; Cl, 13.63; Sn, 22.83. Found: C, 48.79; H, 4.25; N, 11.02; Cl, 13.32; Sn, 23.20%. Selected IR data (CsI, cm^{-1}):1615 s (ν_{tp}), 1543 s (ν_{py}); 540 m ν_{as}(Sn–C); 499 m ν_s (Sn–C); 314 s ν_{as}(Sn–Cl); 269 m ν_s(Sn–Cl). ^1H NMR ($CDCl_3$): δ (ppm) = 8.61(s, 1H, H-2), 7.72 (s, 1H, H-6), 7.67–7.58 (m, 5H, C_6H_5), 8.28–8.13 (m, 5H, C_6H_5), 1.84(q, 4H, Sn–C_2H_5), $^2J(^{119}Sn,H)$: 52.8 Hz, $^2J(^{117}Sn,H)$: 50.8 Hz, 1.45(t, 6H, Sn–C_2H_5), $^3J(^{119}Sn,H)$: 139.0 Hz, $^3J(^{117}Sn,H)$: 132.9 Hz. ^{13}C NMR ($CDCl_3$): δ (ppm) = 155.9 (C-2), 155.7 (C-3a), 162.4 (C-5), 107.2 (C-6), 148.7 (C-7), 128.0,129.6 (C_{ortho}), 129.4, 129.3 (C_{meta}), 131.9, 132.3 (C_{para}), 130.0, 136.3 (C_{ipso}), 20.7(Sn–C_2H_5), 9.7 (Sn–C_2H_5). ^{119}Sn Mössbauer data: δ = 1.54, ΔE = 3.54, $\Gamma\pm$ = 0.80 mm s^{-1}, ∠C–Sn–C = 134°.

2.6.3. $Bu_2SnCl_2(dptp)$ (**10**)

$C_{25}H_{30}Cl_2N_4Sn$ (576.16) (***10***); m.p. 76–78 °C. Anal. Calc.: C, 52.12; H, 5.25; N, 9.72; Cl, 12.31; Sn, 20.60. Found: C, 52.39; H, 5.38; N, 10.03; Cl, 12.37; Sn 20.32%. Selected IR data (CsI, cm^{-1}):1610 s (ν_{tp}), 1542 s (ν_{py}); 687 m ν_{as}(Sn–C); 334 m ν_{as}(Sn–Cl); 281 m ν_s (Sn–Cl). ^1H NMR ($CDCl_3$): δ (ppm) = 8.62 (s, 1H, H-2), 7.73(s, 1H, H-6), 7.67–7.56 (m, 5H, C_6H_5), 8.27–8.13 (m, 5H, C_6H_5), 1.91–1.77 m, 1.42dd, 0.93 t (18H, Sn–nC_4H_9). ^{13}C NMR ($CDCl_3$): δ (ppm) = 155.9 (C-2), 155.8 (C-3a), 162.3 (C-5), 107.1 (C-6), 148.6 (C-7); 128.0,129.6 (C_{ortho}), 129.4, 129.2 (C_{meta}), 131.9, 132.3 (C_{para}), 130.0, 136.3 (C_{ipso}), 26.5, 28.2, 27.3, 13.7 (Sn–nC_4H_9). ^{119}Sn Mössbauer data: δ = 1.49, ΔE = 3.35, $\Gamma\pm$ = 0.83 mm s^{-1}, ∠C–Sn–C = 129°.

2.6.4. $Ph_2SnCl_2(EtOH)_2(dptp)_2$ (**11**)

$C_{50}H_{46}Cl_2N_8O_2Sn$ (980.54) (***11***); m.p. 133–135 °C. Anal. Calc.: C, 61.24; H, 4.73; N, 11.43; Cl, 7.23; Sn, 12.11. Found: C, 60.97; H, 4.27; N, 11.30; Cl, 7.66; Sn 12.41%. Selected IR data (CsI, cm^{-1}):1610 s (ν_{tp}), 1539 s (ν_{py}); 290 m ν_{as}(Sn–C); 249 m ν_{as}(Sn–Cl). ^1H NMR ($CDCl_3$): δ (ppm) = 8.54 (s, 1H, H-2), 7.66 (s, 1H, H-6), 7.48–7.46, 7.64–7.62 (m, 5H, C_6H_5), 8.20–8.09 (m, 5H, C_6H_5), 7.79–7.76 (m, 4H, Sn–C_6H_5 *meta*, 7.55–7.51 (m, 6H, Sn–C_6H_5 *ortho* + *para*); 3.73 (q, 4H, EtOH), 1.25 (t, 6H, EtOH).^{13}C NMR ($CDCl_3$): δ (ppm) = 156.1 (C-2), 156.0 (C-3a), 162.0 (C-5), 106.9 (C-6), 148.4 (C-7), 128.0,129.5 (C_{ortho}), 129.3, 129.2 (C_{meta}), 131.7, 132.1 (C_{para}), 130.1, 136.3 (C_{ipso}), 139.0 (Sn–C_6H_5 *ipso*), 135.2 (Sn–C_6H_5 *ortho*), 129.6 (Sn–C_6H_5 *meta*), 131.7 (Sn–C_6H_5 *para*); 58.6 (CH_2, EtOH), 18.6 (CH_3, EtOH). ^{119}Sn Mössbauer data: δ = 1.26, ΔE = 3.82, $\Gamma\pm$ = 0.83 mm s^{-1}, ∠C–Sn–C = 180°.

2.6.5. $BuSnCl_3(dptp)_2$ (**12**)

$C_{38}H_{33}Cl_3N_8Sn$ (826.81) (***12***); m.p. 125–127 °C. Anal. calc.: C, 55.20; H, 4.02; N, 13.55; Cl, 12.86; Sn, 14.36. Found: C, 55.05; H, 4.14; N, 13.27; Cl, 12.61; Sn 14.90%. Selected IR data (CsI, cm^{-1}):1615 s (ν_{tp}), 1541 s (ν_{py}); 602 m ν(Sn–C); 326w, 296 m 257w,br ν(Sn–Cl). ^1H NMR ($CDCl_3$): δ (ppm) = 8.71 (s, 1H, H-2), 7.76(s, 1H, H-6), 7.69–7.56 (m, 5H, C_6H_5), 8.28–8.09 (m, 5H, C_6H_5), 2.59(m, 4H, Sn–nC_4H_9), 2.02–1.92 (m, 4H, Sn–nC_4H_9),1.50 (m, 4H, Sn–nC_4H_9), 0.92 (t, 6H, Sn–nC_4H_9). ^{13}C NMR ($CDCl_3$): the spectrum not be recorded because of its poor solubility. ^{119}Sn Mössbauer data: δ = 0.98, ΔE = 2.11, $\Gamma\pm$ = 0.83 mm s^{-1}.

3. Results and discussion

3.1. Solid state studies

3.1.1. Crystal structure of $Et_2SnCl_2(dbtp)_2$ (**4**)

The crystal and molecular structure of $Et_2SnCl_2(dbtp)_2$ (***4***) is shown in Fig. 2 together with the crystallographic labeling. Relevant bond distances and angles are reported in Table 2. The molecule is symmetric and the Sn atom sits on a crystallographic glide plane, so that only half a molecule constitutes the asymmetric unit. The Sn atom is hexacoordinate, with the triazolopyrimidine ligand being directly coordinated to the metal and acting as a monodentate ligand through a single nitrogen atom, as often found in compounds provided with a direct metal-triazolopyrimidine bond.

In a series of metal coordinated triazolopyrimidine compounds investigated through X-ray diffraction, the most frequent geometry found in the structural analysis is octahedral with two (or four) triazolo-[1,5-a]pyrimidine ligands monodentately coordinated via the nitrogen atom in position 3, with strong metal-to-N interaction [1]. On the other hand, compound **4** contains two weakly bound triazolopyrimidine ligands and exhibits a highly distorted octahedral geometry of the coordination around the Sn atom, resulting in a C–Sn–C angle of 157.6(2)°. Thus, the overall geometry about the Sn atom is best described as a skew-trapezoidal bipyramid with the tin-bonded carbon atoms of the ethyl groups being bound in pseudo-axial positions over

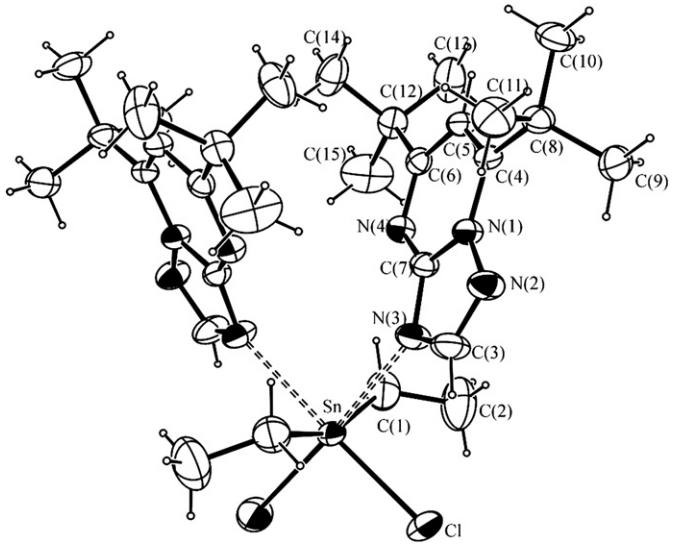

Fig. 2. Crystal structure of $Et_2SnCl_2(dbtp)_2$ (***4***) showing the crystallographic numbering (ORTEP at 30% probability).

Table 2
Selected bond lengths (Å) and angles (°).

Compound **4**[a]	Compound **11**[b]
Sn–C(1) 2.114(4)	Sn–C(1) 2.1441(13)
Sn–N(3) 2.603(2)	Sn–O(1) 2.2705(19)
Sn–Cl(1) 2.4640(8)	Sn–Cl(1) 2.5383(7)
C(1)–Sn–C(1) 157.56(19)	C(1)–Sn–C(1) 180.0
C(1)–Sn–N(3) 82.91(10)	C(1)–Sn–O(1) 90.58(8)
C(1)–Sn–N(3) 81.38(11)	C(1)–Sn–O(1) 89.42(8)
N(3)–Sn–N(3) 90.80(10)	O(1)–Sn–O(1) 180.0
C(1)–Sn–Cl(1) 95.08(9)	C(1)–Sn–Cl(1) 89.36(5)
C(1)–Sn–Cl(1) 99.64(10)	C(1)–Sn–Cl(1) 90.64(5)
Cl(1)–Sn–N(3) 85.75(5)	O(1)–Sn–Cl(1) 91.73(6)
Cl(1)–Sn–N(3) 176.24(5)	O(1)–Sn–Cl(1) 88.27(6)
Cl(1)–Sn–Cl(1) 97.73(5)	C(1)–Sn–Cl(1) 90.64(5)
	C(1)–Sn–Cl(1) 89.36(5)
	O(1)–Sn–Cl(1) 88.27(6)
	O(1)–Sn–Cl(1) 91.73(6)
	Cl(1)–Sn–Cl(1) 180.0

[a] Symmetry transformations used to generate equivalent atoms: I 1/2-x, y, -z.
[b] Symmetry transformations used to generate equivalent atoms: I 1-x, 1-y, -z.

the weaker equatorial Sn–Cl and Sn–N interactions [2.464(1) and 2.603 (2)Å, respectively]. Although this latter Sn – N bond distance is quite long, it is considerably less than the sum of their van der Waals radii (3.75 Å), therefore it should be considered as a bonding interaction. The angle at the tin atom formed between N(1) and Cl(1), 176.2(2)°, is indicative of the *trans* positions of the ligands, while the *cis* ligands, Cl–Sn–C(1) angle is significantly widened to 99.6(1)°, Cl–Sn–Cl is also widened to 97.7(1)° while N(1)–Sn–C(1) is 82.9(1)°.

Supramolecular organization: The reason for the highly distorted octahedral geometry around the Sn atom can be explained taking into account the supramolecular organization of the compound. Actually, non-conventional H-bonding interactions between hydrogen atoms belonging to –CH methyl groups of one molecule and Cl atoms of a second one (Cl···H–C distance 2.91 (1) Å, D···A distance 3.857(3)Å, Cl···H–C angle 171.1(1)°) create an infinite polymeric arrangements of molecules forming rows of columns elongated along the *c* axis, shown in Fig. 3 (a) in wires (H-bonds in dotted lines) and in spacefill representation, Fig. 3 (b). Moreover, a further stabilization is given by some intramolecular C–H···N interactions and a π-stacking aromatic intramolecular interaction occurring between the two symmetry-related six-membered pyrimidine rings which lay 4.7 Å apart from each other. The two rings may be defined as inclined, making an angle of 40° between their mean planes, according to the geometries of aromatic interactions defined by Aravinda et al. for peptide scaffolds [30].

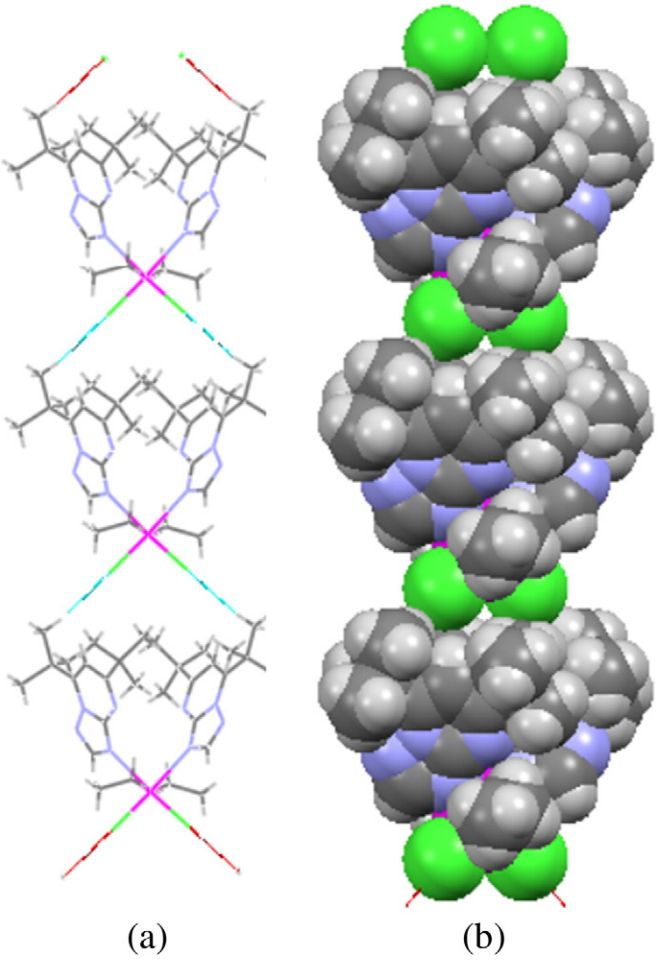

Fig. 3. Packing of $Et_2SnCl_2(dbtp)_2$ (***4***) viewed along the *c* axis.

3.1.2. Crystal structure of $Ph_2SnCl_2(EtOH)_2(dptp)_2$ (**11**)

In $Ph_2SnCl_2(EtOH)_2(dptp)_2$ (***11***), whose structure is shown in Fig. 4, the tin atom sits on a crystallographic inversion center and, also in this case, only half a molecule constitutes the crystallographic independent unit. The ligands at Sn(IV) are two phenyl rings and two chlorine atoms. The octahedral geometry is completed by two ethanol molecules which coordinate the Sn atom through their oxygen atoms, which coordinate further two **dptp** molecules, not directly connected to the metal centre but H-bonded in a quite strong interaction [O···N distance 2.698(3) , O–H···N angle 175(1)°] through the triazole N (3) atom. In addition, the **dptp** molecules are more loosely held *via* a second H-bond interaction trough the pyrimidine N(4) and one H atom belonging to the terminal methyl group, C(25). According to literature data [1], a few compounds have been described in which

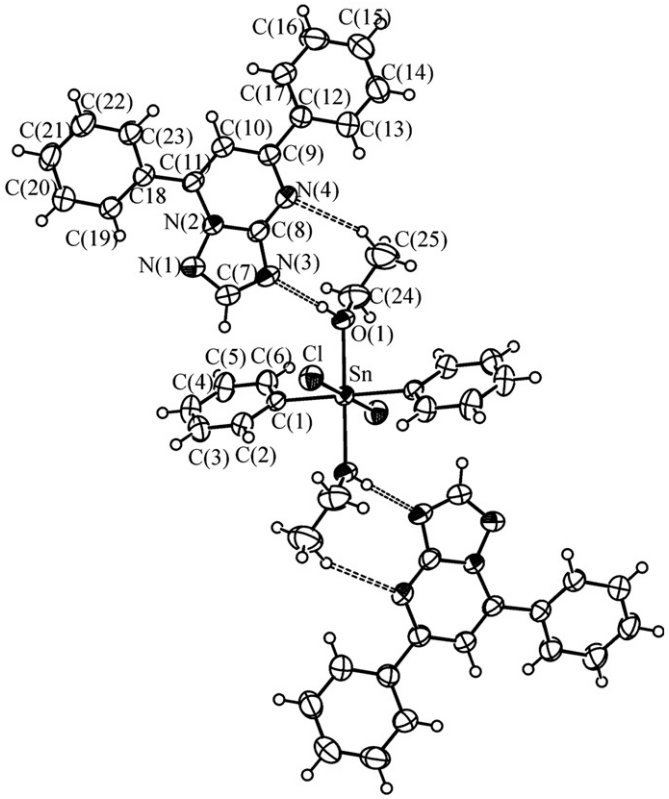

Fig. 4. Molecular structure of $Ph_2SnCl_2(EtOH)_2(dptp)_2$ (***11***) showing the crystallographic labeling of the independent part of the molecule (ORTEP at 50% probability).

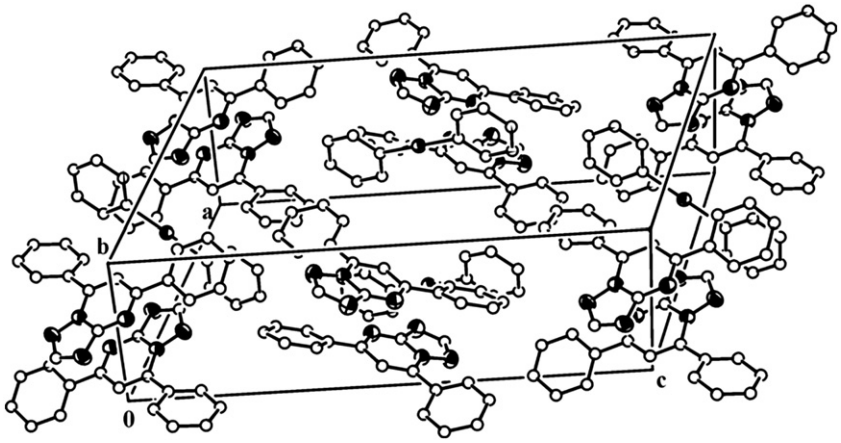

Fig. 5. Packing of $Ph_2SnCl_2(EtOH)_2(dptp)_2$ (***11***), showing the π stacking of the triazolo pirimidine pairs and the aromatic–aromatic interactions (chlorine and ethanol ligands and hydrogen atoms have been omitted for clarity).

there is no direct bond between the metal atom and the triazolopyrimidine derivative. When the dmtp is protonated at N(3) behaving as a counterion of a complex such as $[SnCl_6]^{2-}$ [31] cations associate in hydrogen bonded N(3)–H···N(4) couples, confirming the fact that N(3) and N(4) positions are the most common sites for bidentate coordination. In **11**, the Sn–Cl distance, 2.538(1) Å, *trans* to the same weak-field chlorine ligand, is considerably longer than the one found in **4**, Sn–Cl(1) 2.4640(8) Å, *trans* to the N(3) of the triazolo moiety. Also in $Ph_2SnCl_2L{\cdot}EtOH$ [32] (where L = 3-methyl-2-hydroxy-2-cyclopenten-1-one), the metal-to-chlorine interaction is 2.313(1) Å, having an O-bound ethanol molecule as a *transoid* ligand [Cl–Sn–O 166.1(1)°], due to the increased π-acceptor properties of the ligand. Consistently, in **11,** the Sn–O (ethanol) interaction, 2.271(1) Å, *trans* to itself, appears again considerably longer than the value, 2.118(3) Å, found in the previously mentioned in $Ph_2SnCl_2L{\cdot}EtOH$ complex [32]. The dihedral angle between the strictly planar triazolopyrimidine moiety [max deviation from planarity for C(9), 0.0270 Å] and the plane containing Sn, Cl(1) and O(1) is 50.08°, while the angle between the **tp** moiety and the Sn-bound phenyl ring [C(1) to C(6)] is 68.36°**.** Strong π-stacking "antiparallel" interactions between pairs of triazolopyrimidine moieties, related by the C_i symmetry operator, occur with a centroid–centroid distance of 3.7 Å. In addition to these, a close network of edge-to-face and π-stacking interactions involving all the aromatic rings present in the molecule [CH-centroid and centroid–centroid distances in the range of 4.2–4.4 Å] contributes to a further stabilization of the structure (Fig. 5).

3.1.3. IR spectra and Mössbauer data

The IR spectra of the complexes have been examined in comparison with the spectra of the free ligands [33]. The two most characteristic bands in the IR spectra of **dbtp** and **dptp**, assigned to an overall triazolopyrimidine and pyrimidine ring mode vibrations, ν_{tp} (1615 and 1612 cm^{-1}) and ν_{py} (1530 and 1543 cm^{-1}), are generally moved to higher frequencies in transition metal complexes [34,35]. In the organotin(IV) derivatives under investigation, not significant shift on coordination is found, presumably due to the extensive hydrogen bonds network in both ligand [36] and investigated compounds. The only differences in the spectra are due to ν(Sn–C) and ν(Sn–Cl) stretching vibrations in the low-frequency region [37,38]. The values of the Mössbauer quadrupole splittings parameters give very useful information on the solid-state structure of the diorganotin(IV) complexes as they can be related to the geometry of the diorganotin(IV) moiety: the C – Sn – C bond angle in such compounds can be simply estimated through "point-charge" calculations assuming that the quadrupole splitting is set up just by the R_2Sn unit, the contribution to the electric field gradient on the tin nucleus being dominated by the highly covalent Sn – C bonds [39]. Hence, idealized octahedral and *cis*-R_2 trigonal bipyramidal structures for $R_2SnCl_2L_2$ and R_2SnCl_2L complexes, respectively, are proposed (L = **dbtp** or **dptp**). Using the partial quadrupole splitting (p.q.s.) values [40] −1.03 and −1.13 mm s^{-1} [41] for octahedral and equatorial trigonal bipyramidal alkyl groups respectively, and −0,95 and −0.98 mm s^{-1} for the corresponding phenyl groups, the C – Sn – C bond angles were estimated as reported under the analitical data. As far as the 1:1 complexes are concerned, compounds **1**, **3**, **6**, **9**, and **10**, the estimated C – Sn – C bond angles are in the range 125–134° according to a distorted *cis*-R_2 tbp structure (Fig. 6a). Among the 1:2 complexes, **8** and **11** are characterized by an essentially linear C–Sn–C fragment (Fig. 6b), according to the presence of only one ν(Sn–C) band in the infrared spectrum of **8**, and, most of all, to the X-ray all-trans structure of **11**. The **dbtp** derivatives **2**, **4** and **5** are characterized by quite similar Mössbauer spectra which suggests distorted octahedral structures (Fig. 6c), with C – Sn – C bond angles lower than 180°. The estimated angle for $Et_2SnCl_2(dbtp)_2$ (***4***) is virtually identical to that determined by X-ray diffraction, showing that for this class of compounds the method can be considered particularly efficient. As far as the monoorganotin (IV) derivatives **7** and **12** are concerned, we may only observe that the quadrupole splitting values are consistent with octahedral structures.

3.2. Solution state studies

3.2.1. ^1H and ^{13}C NMR spectra

Structural informations for the complexes in solution have been acquired by ^1H, ^{13}C and ^1H–^1H COSY (correlation spectroscopy) spectra. ^1H and ^{13}C NMR relevant resonances for the free ligands and the complexes performed in $CDCl_3$ (see Experimental section). The ^1H resonances of the **dbtp** ligand are assigned according to Szlyk [42]; assignments of **dptp** resonances in $CDCl_3$ (8.55 ppm for H(2), 7.68 ppm for H(6), 7.65–7.55 and 8.29–8.12 ppm for C_6H_5 group) and for ^{13}C NMR spectra are in agreement with those reported by Grodzicki [29] in DMSO-d_6. The ^1H NMR spectra for the novel **dbtp** complexes present two characteristic singlet signals of H(2) and H(6) in the range 7.01–8.72 ppm, and similarly resonances for **dptp** are in the range 7.66–8.71 ppm. The spectra are slightly modified, with the same multiplicity of signals, with respect to the ligands. The coordination of triazolopyrimidine derivatives by organotin(IV) results in the downfield shift of H(2) and H(6) resonances. Coordination *via* N(3) slightly affects the ^{13}C spectrum of the ligands: the carbons adjacent to N(3) coordination site, *i.e.* C(2) and C(3a) are shifted upfield whereas those of C(5), C(6) and C(7) are moved in the opposite direction. Coordination *via* N(3) of these two ligands is in agreement with similar results presented for platinum(II) and palladium (II) chloride complexes [35]. As for the organometallic moieties, ^1H

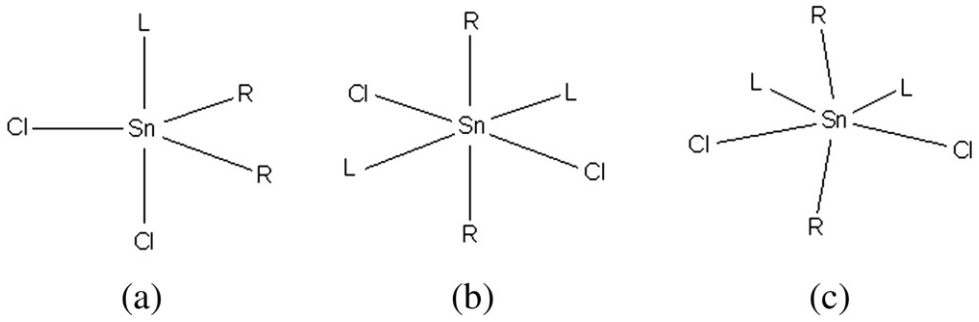

Fig. 6. Proposed structures for R_2SnL and R_2SnL_2 complexes: (a) R = Me, Et, Ph; L = dbtp; R = Et, *n*-Bu; L = dptp. (b) L = Me, Ph; L = dptp. (c) R = Me, Et, *n*-Bu; L = dbtp.

NMR spectra for Me_2SnCl_2(dbtp) (***1***) and $Me_2SnCl_2(dbtp)_2$ (***2***) complexes, present a single resonance at 1.30 and 1.31 ppm, respectively. Lockhart and Manders' relationship [43] between C–Sn–C bond angles and $|^2J|$ can be applied. For Me_2SnCl_2(dbtp) (***1***), $|^2J(^{119}Sn, ^1H)|$ being 78.8 Hz, the calculated C–Sn–C bond angle is 129.3° while in $Me_2SnCl_2(dbtp)_2$ (***2***), $|^2J(^{119}Sn, ^1H)|$ being 80.4 Hz, a C–Sn–C bond angle of 131.4° was obtained. There are no significant differences between the Me_2SnCl_2(dbtp) and $Me_2SnCl_2(dbtp)_2$ complexes, which suggests that even in a non-coordinating solvent solution, a ligand unit has been displaced. A similar trend has been observed following the comparison between Et_2SnCl_2(dbtp) and $Et_2SnCl_2(dbtp)_2$ complexes, $|^2J(^{119}Sn, ^1H)|$ being 57.8 Hz, the calculated C–Sn–C bond angle is 110.9° and $|^2J(^{119}Sn, ^1H)|$ being 58.6 Hz, the calculated C–Sn–C bond angle is 111.3°, respectively. For the complex $Me_2SnCl_2(dptp)_2$ (***8***), $|^2J(^{119}Sn, ^1H)|$ being 77.4 Hz, the calculated C–Sn–C bond angle is 127.7°, while for Et_2SnCl_2(dptp) (***9***), $|^2J(^{119}Sn, ^1H)|$ being 52.8 Hz, the calculated C–Sn–C bond angle is 108.6°. The aromatic proton resonances of Ph_2SnCl_2(dbtp) (***6***) are found in two groups at 7.76–7.73 ppm (corresponding to four protons) which are observed at lower fields due to *ortho* hydrogens of the phenyl groups attached to tin, and 7.48 ppm (corresponding to six protons) as multiplets due to *meta* and *para* hydrogens [44]. For $Ph_2SnCl_2(EtOH)_2(dptp)_2$ (***11***) whose resonance assignments are reported under Experimental, $^1H–^1H$ COSY spectrum is presented in Fig. 7. In all NMR spectra sharpness of resonances gives an indication that fluxionality is absent, even for coordinated ethanol molecules in **11**.

3.3. Antimicrobial activity

The compounds were screened for their *in vitro* antibacterial activity on a group of reference staphylococcal strains susceptible or resistant to methicillin and against two reference Gram-negative pathogens. The antibacterial activity of the substances, expressed as MIC, is reported in Table 3. The free ligands **dbtp** and **dptp** resulted inactive at the maximum tested concentration of 100 μg mL^{-1}, whereas organotin(IV) complexes show a better antibacterial activity against Gram-positive strains. $Ph_2SnCl_2(EtOH)_2(dptp)_2$ (***11***) and *n*-$Bu_2SnCl_2(dbtp)_2$ (***5***) showed good antibacterial activity with a MIC value of 5 and 10 μg mL^{-1} respectively against *S. aureus* ATCC29213 and the compound *n*-$Bu_2SnCl_2(dbtp)_2$ (***5***) showed an interesting activity, (MIC value of 20 μg mL^{-1}) against the methicillin resistant strain *S. aureus* ATCC43866 too. Ph_2SnCl_2(dbtp) (***6***), $Ph_2SnCl_2(EtOH)_2(dptp)_2$ (***11***), *n*-Bu_2SnCl_2(dptp) (***10***) and *n*-$BuSnCl_3(dbtp)_2$ (***7***) resulted active against methicillin resistant *S. epidermidis* RP62A, but unfortunately showed a weak or no activity against the other strains. However, none of the compounds resulted active against all the tested staphylococcal strains. The significative antibacterial properties of the above mentioned organotin (IV) complexes, among these, most active being Ph_2SnCl_2 and *n*-Bu_2SnCl_2 derivatives, were encouraging. Inhibitory activity increases in the order Me ~ Et < *n*-Bu < Ph and is attributed to lipophilicity, following the same trend, which facilitates microorganism membrane crossing, in agreement with the knowledge that the toxicity of the organotins is related to their hydrophobicity [45,46]. A qualitative structure-activity relationship can tentatively be advanced, where coordination environment of the tin atom is crucial: six-coordinated tin complex, $Ph_2SnCl_2(EtOH)_2(dptp)_2$ (***11***), displayed better results than the five-coordinated Ph_2SnCl_2(dbtp) one (***6***) against *S. aureus* ATCC 29213. The extensive hydrogen bonds network which is present in the former [36] is indicative of the potential mode action of this compound which could be described in terms of hydrogen bonding with the active centers of the cell constituents, resulting in an interference, with the normal cell processes. All the complexes and the parent compounds showed poor activity against Gram-negative reference strains, with the exception of Et_2SnCl_2, which showed a MIC value of 40 μg mL^{-1} against *P. aeruginosa* ATCC9027 and *E. coli* ATCC25922. The complexes Et_2SnCl_2(dbtp) (***3***), $Et_2SnCl_2(dbtp)_2$ (***4***) and Et_2SnCl_2(dptp) (***9***), exhibited antibacterial properties less potent than the parent organotin(IV) compounds. As an overall result, the complexes were more toxic towards Gram-positive than Gram-negative strains; the reason laying in the different structures of cell walls, which in Gram-negative cells are more complex than those in the Gram-positive ones [12].

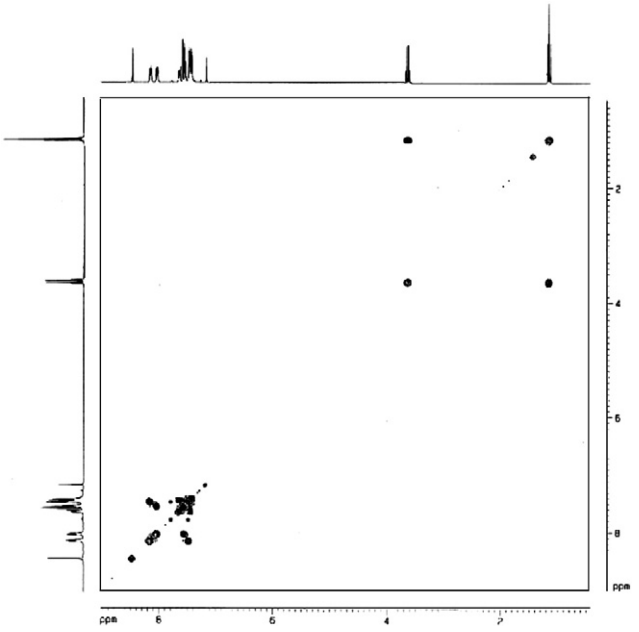

Fig. 7. $^1H–^1H$ COSY spectrum for $Ph_2SnCl_2(EtOH)_2(dptp)_2$.

Table 3
Anti-staphylococcal activity *in vitro*, MIC values in μg mL^{-1}.

Compound	*S. aureus* ATCC 29213	*S. aureus* ATCC 25923	*S. aureus* ATCC 43866	*S. epidermidis* RP62A
Me_2SnCl_2	>40	[a]	>40	>40
$Me_2SnCl_2 \cdot$ dbtp (***1***)	>40	>40	>40	>40
$Me_2SnCl_2(dbtp)_2$ (***2***)	>40	>40	>40	>40
$Me_2SnCl_2(dptp)_2$ (***8***)	>40	>40	>40	>40
Et_2SnCl_2	20	[a]	20	20
Et_2SnCl_2(dbtp) (***3***)	>40	>40	>40	>40
$Et_2SnCl_2(dbtp)_2$ (***4***)	>40	>40	>40	>40
Et_2SnCl_2(dptp) (***9***)	>40	>40	>40	>40
n-Bu_2SnCl_2	40	[a]	>40	>40
n-$Bu_2SnCl_2(dbtp)_2$ (***5***)	10	>40	20	>40
n-Bu_2SnCl_2(dptp) (***10***)	40	>40	>40	10
Ph_2SnCl_2	20	[a]	>40	1.2
Ph_2SnCl_2(dbtp) (***6***)	20	>40	>40	5
$Ph_2SnCl_2(EtOH)_2(dptp)_2$ (***11***)	5	>10	>10	5
n-$BuSnCl_3$	>40	>40	>40	1.2
n-$BuSnCl_3(dbtp)_2$ (***7***)	>20	>20	>20	20
n-$BuSnCl_3(dptp)_2$ (***12***)	>40	>40	>40	>40
dbtp	>100	>100	>100	>100
dptp	>100	>100	>100	>100
Amikacin	1.2	[a]	1.2	1.2

[a] MIC value published on reference [8].

4. Conclusions

A considerable series (twelve novel compounds are reported) of 5,7-ditertbutyl-1,2,4-triazolo[1,5-a]pyrimidine (**dbtp**) and 5,7-diphenyl-1,2,4-triazolo[1,5-a]pyrimidine (**dptp**) were synthesized and investigated by FT-IR and ^{119}Sn Mössbauer in the solid state and by ^{1}H and ^{13}C NMR spectroscopy, in solution. The X-ray crystal and molecular structures of $Et_2SnCl_2(dbtp)_2$ (***4***) and $Ph_2SnCl_2(EtOH)_2(dptp)_2$ (***11***) were described. The main result of the structural investigations of complexes **4** and **1** lies in the network of hydrogen bonding and aromatic interactions involving pyrimidine and phenyl rings. Non-covalent interactions involving aromatic rings are key processes in both chemical and biological recognition, contributing to overall complex stability and forming recognition motifs. It is noteworthy that in complex **11**, π–π stacking interactions between pairs of antiparallel triazolopyrimidine rings mimick base-pair interactions physiologically occurring in DNA.

As for the antimicrobial activity, the latter being very active with a MIC value of 5 μg mL^{-1} against *S. aureus* ATCC29213. *n*-Bu_2SnCl_2(dptp) and *n*-$BuSnCl_3(dbtp)_2$ resulted active against methicillin resistant *S. epidermidis* RP62A, but showed a weak or no activity against the other strains. Unfortunately, we are forced to conclude that substitution in the ligands of hydrogen (**tp**) and methyl (**dmtp**) with tert-butyl (**dbtp**) and phenyl (**dptp**) groups, affords complexes whose activity against *S. aureus* ATCC 25923, exhibit a lower inhibition against bacteria, which clearly indicates that introduction of sterically hindering organic residues decreases the activity of the parent organometallic moieties. This notwithstanding, an overall view on the biological activity of this class of molecules is attractive, and a rational development of leads including modified entities, endowed with more effective antimicrobial properties, according to the basic principles outlined by Silverman [47], can be pursued.

Acknowledgment

Financial support by the Ministero dell'Istruzione, dell'Università e della Ricerca, Rome and by the Università degli Studi di Palermo is gratefully acknowledged.

Appendix A. Supplementary data

Supplementary data to this article can be found online at doi:10.1016/j.jinorgbio.2011.09.010.

References

[1] J.M. Salas, M.A. Romero, M.P. Sanchez, M. Quiros, Coord. Chem. Rev. 193 (1999) 1119–1142.
[2] Jaap G. Haasnoot, Coord. Chem. Rev. 200–202 (2000) 131–185.
[3] E. Szłyk, A. Wojtczak, M. Jaskólski, M. Gilski, J.G. Haasnoot, J. Reedijk, Inorg. Chim. Acta 260 (1997) 145–150.
[4] C.R. Maldonado, M. Quirós, J.M. Salas, Polyhedron 27 (2008) 2779–2784.
[5] I. Łakomska, Inorg. Chim. Acta 362 (2009) 669–681.
[6] J.M. Balkaran, S.C.P. van Bezouw, J. van Bruchem, J. Verasdonck, P.C. Verkerk, A.G. Volbeda, I. Mutikainen, U. Turpeinen, G.A. van Albada, P. Gamez, J.G. Haasnot, J. Reedijk, Inorg. Chim. Acta 362 (2009) 861–868.
[7] M.A. Girasolo, C. Di Salvo, D. Schillaci, G. Barone, A. Silvestri, G. Ruisi, J. Organomet. Chem. 690 (2005) 4773–4783.
[8] M.A. Girasolo, D. Schillaci, C. Di Salvo, G. Barone, A. Silvestri, G. Ruisi, J. Organomet. Chem. 691 (2006) 693–701.
[9] G. Ruisi, L. Canfora, G. Bruno, A. Rotondo, T.F. Mastropietro, E.A. Debbia, M.A. Girasolo, B. Megna, J. Organomet. Chem. 695 (2010) 546–551.
[10] S. Tabassum, C. Pettinari, J. Organomet. Chem. 691 (2006) 1761–1766.
[11] S.K. Hadjikakou, N. Hadjiliadis, Coord. Chem. Rev. 253 (2009) 235–249.
[12] T.S. Basu Baul, Appl. Organomet. Chem. 22 (2008) 195–204.
[13] M. Nath, H. Singh, P. Kumar, A. Kumar, X. Song, G. Eng, Appl. Organomet. Chem. 23 (2009) 347–358.
[14] A.B. Caballero, C. Marín, A. Rodríguez-Diéguez, I. Ramírez-Macías, E. Barea, M. Sánchez-Moreno, J.M. Salas, J. Inorg. Biochem. 105 (2011) 770–776.
[15] I. Ramírez-Macías, C. Marín, J.M. Salas, A. Caballero, M.J. Rosales, N. Villegas, A. Rodríguez-Diéguez, E. Barea, M. Sánchez-Moreno, J. Antimicrob. Chemother. 66 (2011) 813–819.
[16] A.B. Caballero, C. Marín, O. Huertas, A. Rodríguez-Diéguez, J.M. Salas, M. Sánchez-Moreno, CO10 of VII Reunión Científica de Bioinorgánica, Águilas (Murcia) Spain, 3–6 july, 2011.
[17] Y.W. Tang, C.W. Stratton, Clin. Lab. Med. 30 (1) (2010) 179–208.
[18] K. Ohlsen, U. Lorenz, Future Microbiol. 2 (2007) 655–666.
[19] W. Schöniger, Mikrochim. Acta (1955) 123–129.
[20] A. Barbieri, G. Ruisi, A. Silvestri, A.M. Giuliani, A. Barbieri, G. Spina, F. Pieralli, F. Del Giallo, J. Chem. Soc., Dalton Trans. (1995) 467–475 and refs. therein.
[21] G.M. Sheldrick, SADABS, University of Göttingen, Germany, 1996.
[22] SMART & SAINT Software Reference Manuals, version 5.051 (Windows NT Version), Bruker Analytical X-ray Instruments Inc, Madison, Wi, 1998.
[23] G.M. Sheldrick, SHELXS-97, University of Göttingen, Germany, 1997.
[24] G.M. Sheldrick, SHELXL-97, University of Göttingen, Germany, 1997.
[25] L.J. Farrugia, ORTEP-3 for Windows: a version of *ORTEP*-III with a Graphical User Interface, J. Appl. Crystallogr. 30 (1997) 565.
[26] C.F. Macrae, I.J. Bruno, J.A. Chisholm, P.R. Edgington, P. McCabe, E. Pidcock, L. Rodriguez-Monge, R. Taylor, J. van de Streek, P.A. Wood, J. Appl. Crystallogr. 41 (2008) 466–470.
[27] L.J. Farrugia, J. Appl. Crystallogr. 32 (1999) 837–838.
[28] D. Schillaci, S. Petruso, V. Sciortino, Int. J. Antimicrob. Agents 25 (2005) 338–340.
[29] A. Grodzicki, E. Szlyk, A.L. Pazderski, A. Goliński, Magn. Reson. Chem. 34 (1996) 725–737.
[30] S. Aravinda, N. Shamala, C. Das, A. Sriranjini, I.L. Karle, P. Balaram, J. Am. Chem. Soc. 125 (2003) 5308–5315.
[31] J.M. Salas, A. Rahmani, M.A. Romero, A.D. Rae, A.C. Willis, E.R.T. Tiekink, Z. Krist. 213 (1998) 302–304.
[32] C. Camacho-Camacho, V.M. Jiménez-Pérez, J.C. Galvez-Ruiz, A. Flores-Parra, R. Contreras, J. Organomet. Chem. 691 (2006) 1590–1597.
[33] E. Szłyk, A. Grodzicki, L. Pazderski, J. Sitkowski, Pol. J. Chem. 72 (1998) 55–60.
[34] I. Łakomska, E. Szłyk, J. Sitkowski, L. Kozerski, J. Wietrzyk, M. Pełczynska, A. Nasulewicz, A. Opolski, J. Inorg. Biochem. 98 (2004) 167–172.
[35] I. Łakomska, M. Barwiołek, A. Wojtczak, E. Szłyk, Polyhedron 26 (2007) 5349–5354.
[36] A. Surdykowski, E. Szłyk, S. Larsen, Acta Crystallogr. C55 (1999) 1337–1339.
[37] R.J.H. Clark, C.S. Williams, Spectrochim. Acta 21 (1965) 1861–1868.
[38] C. Pettinari, F. Marchetti, A. Cingolani, S. Bartolini, Polyedron 15 (1996) 1263–1276.
[39] R.V. Parish, in: G.J. Long (Ed.), Mössbauer Spectroscopy Applied to Inorganic Chemistry, Plenum Press, New York, 1984, pp. 527–575.
[40] G.M. Bancroft, R.H. Platt, Adv. Inorg. Chem. Radiochem. 15 (1972) 59–258.
[41] G.M. Bancroft, V.G. Kumar Das, T.K. Sham, M.G. Clark, J. Chem. Soc., Dalton Trans. (1976) 643–654.
[42] E. Szłyk, A. Grodzicki, L. Pazderski, A. Wojtczak, J. Chatlas, G. Wrzeszcz, J. Sitkowski, B. Kamieński, J. Chem. Soc. Dalton Trans. (2000) 867–872.
[43] T.P. Lockart, W.F. Manders, Inorg. Chem. 25 (1986) 892–895.
[44] M.K. Das, S. De, J. Organomet. Chem. 495 (1995) 177–184.
[45] S. Ianelli, M. Orcesi, G. Pelizzi, F. Zani, J. Inorg. Biochem. 60 (1995) 89–108.
[46] J.J. Cooney, S. Wuertz, J. Ind. Microbiol. Biotechnol. 4 (1989) 375–402.
[47] R.B. Silverman, in: Elsevier (Ed.), The Organic Chemistry of Drug Design and Drug Action, Academic Press, London, 2004, pp. 7–120.